

Smooth termination of intruder bands in $^{109}_{51}\text{Sb}$

H. Schnare,^{*} D. R. LaFosse,[†] D. B. Fossan, J. R. Hughes,[‡] and P. Vaska
Department of Physics, State University of New York at Stony Brook, Stony Brook, New York 11794

K. Hauschild, I. M. Hibbert, and R. Wadsworth
Department of Physics, University of York, Heslington, York YO1 5DD, United Kingdom

V. P. Janzen and D. C. Radford
Chalk River Laboratories, Atomic Energy of Canada Limited, Chalk River, Ontario, Canada K0J 1J0

S. M. Mullins[§]
Department of Physics and Astronomy, McMaster University, Hamilton, Ontario, Canada L8S 4M1

C. W. Beausang and E. S. Paul
Oliver Lodge Laboratory, University of Liverpool, P.O. Box 147, Liverpool L69 3BX, United Kingdom

J. DeGraaf
Department of Physics, University of Toronto, Toronto, Ontario, Canada M5S 1A7

I.-Y. Lee and A. O. Macchiavelli
Nuclear Science Division, Lawrence Berkeley National Laboratory, Berkeley, California 94720

A. V. Afanasjev,^{||} and I. Ragnarsson
Department of Mathematical Physics, University of Lund, P.O. Box 118, S-22100 Lund, Sweden
 (Received 8 February 1996)

Intruder rotational bands have been investigated to high frequency in $^{109}_{51}\text{Sb}$. Five decoupled ($\Delta I=2$) bands extending to rotational frequencies above 1.4 MeV/ \hbar have been observed. At the highest frequencies, the $\mathcal{J}^{(2)}$ dynamic moments of inertia for four of these bands are seen to decrease steadily to unexpectedly low values, $\mathcal{J}^{(2)} \sim 10 \hbar^2 \text{MeV}^{-1}$. These four bands, which are interpreted as being based on deformed 2p-2h proton excitations across the $Z=50$ closed-shell gap, achieve the so-called ‘‘smooth band termination’’ following alignment of the valence nucleons outside of ^{100}Sn . In addition, two strongly coupled ($\Delta I=1$) bands have been observed, which are related to 1p-1h proton excitations across the gap. [S0556-2813(96)06010-4]

PACS number(s): 21.10.Re, 23.20.Lv, 27.60.+j

I. INTRODUCTION

Nuclei near the $Z=50$ closed proton shell exhibit collective structure that coexists with the expected single-particle structure. Intruder rotational bands have recently been observed in $Z=50$ to 53 nuclei up to unusually high frequencies. These collective structures involve particle-hole proton excitations (1p-1h, 2p-2h, etc.) across the $Z=50$ shell gap via the $\pi g_{7/2} - \pi g_{9/2}$ level crossing at prolate deformations, which appears to stabilize deformed core configurations. At

higher frequencies as additional particle alignment takes place, most of these intruder bands display the unique characteristic of gradually decreasing dynamic moments of inertia with increasing spin to unusually low values, less than a third of the rigid-body value. This structure feature has been interpreted using configuration-dependent cranking calculations [1,2], which showed that as the available valence nucleons outside of the $Z=N=50$ double shell closure align, the nuclear shape gradually traces a path through the triaxial γ plane from a collective prolate shape ($\gamma=0^\circ$) to the noncollective oblate shape ($\gamma=+60^\circ$) over many transitions; this feature is called ‘‘smooth band termination.’’ After the available valence particles for a specific yrast configuration have aligned, the band sequence terminates at a spin that exhausts the sum of the aligned single-particle spins.

Collectivity in the $Z=50$ region was initially observed in the $Z=51$ odd- A Sb isotopes [3], which involved 1p-1h excitations across the shell gap, namely deformed 2p1h configurations, with the β -upsloping $\pi g_{9/2}$ orbital intruding from below the $Z=50$ proton shell. These high- K $9/2^+$ states $\pi(g_{7/2}d_{5/2})^2(g_{9/2})^{-1}$ of modest prolate deformation give rise to strongly coupled ($\Delta I=1$) rotational bands, the bandheads

^{*}Present address: Research Center Rossendorf, PF 510119, D-01314 Dresden, Germany.

[†]Present address: Chemistry Dept., Washington Univ., St. Louis, MO 63130.

[‡]Present address: Lawrence Livermore Laboratory, P.O. Box 808, Livermore, CA 94550.

[§]Present address: Dept. of Nuclear Physics, The Australian National University, Canberra ACT 0200, Australia.

^{||}Permanent address: Nuclear Research Center, Latvian Academy of Sciences, LV-2169, Salaspils, Miera str. 31, Latvia.

of which achieve a minimum excitation energy near the middle of the $N=50-82$ neutron shell. Subsequently, related deformed $2p2h$ 0_2^+ states, $[\pi(g_{7/2}d_{5/2})^2(g_{9/2})^{-2}]$, were discovered [4] via rotational bands in the even- A Sn isotopes, which achieved the lowest energy in ^{116}Sn at $N=66$, the neutron midshell. An investigation in ^{117}Sb [5] revealed collective structure at modest spins, involving the coupling of these $2p2h$ Sn-core deformed states to the $Z=51$ low- K valence proton orbitals. In addition to the $2p1h$ collectivity, three decoupled $\Delta I=2$ rotational bands associated with the $g_{7/2}$, $d_{5/2}$, and $h_{11/2}$ valence proton orbitals coupled to the deformed $2p2h$ ^{116}Sn core band were found in ^{117}Sb rising out of the complicated spherical (single-particle) structure. These results suggest that the $Z=51$ nuclei have a full complement of deformed collective structure involving the $2p2h$ deformed core along with the spherical structure. The $\pi g_{7/2} - \pi g_{9/2}$ level crossing at a quadrupole deformation $\beta_2 \approx 0.2$ strongly influences the proton particle-hole deformed core configurations at low frequencies. The observation in ^{113}Sb [6] of the yrast band based on the $\pi h_{11/2}$ orbital to high spin, $75/2 \hbar$, and high rotational frequency, $\hbar\omega \approx 1.0$ MeV, with an enhanced quadrupole deformation, $\beta_2 \approx 0.3$, revealed multiparticle alignment and strong n-p interactions in these collective structures near $Z=50$. The experiment, which discovered the unique intruder-band properties in the $Z=50$ region, was performed with the 8π spectrometer at Chalk River; both ^{109}Sb [7] and ^{108}Sn [8] revealed three intruder bands to high frequency with gradually decreasing moments of inertia. The theoretical interpretation of these properties in terms of the ‘‘smooth band termination’’ was initiated for ^{109}Sb [1,7] and later developed [2] for other nuclei in this region.

In order to investigate these intruder bands and this termination feature more thoroughly, the improved resolving power of the third-generation GAMMASPHERE array has been employed. The improved sensitivity has been essential to experimentally examine the predicted terminating transitions at the top of the intruder bands. The $Z=51$ ^{109}Sb nucleus, the best example of this structure feature found to date, was studied with the early implementation (EI) of GAMMASPHERE via the $^{54}\text{Fe}(^{58}\text{Ni},3p)$ reaction at a beam energy of 243 MeV. The current paper presents the results of this experiment, which we suggest, extend the three known bands to termination, and revealed two intruder bands. Theoretical calculations for ‘‘smooth band termination,’’ based on the cranked Nilsson-Strutinsky method, are also presented and compared with the experimental results. A preliminary report of these results has been made [9]. The $4p$ and $2p\alpha$ reaction channels in this GAMMASPHERE experiment also provided information on terminating intruder bands in ^{108}Sn [10] and ^{106}Sn [11], respectively. Other related experimental investigations of intruder bands in this region have been carried out in ^{111}Sb [12], $^{112,114}\text{Te}$ [13,14], ^{113}I [15,16], ^{115}I [17], and ^{117}I [18].

II. EXPERIMENTAL DETAILS

The high-spin properties of ^{109}Sb have been investigated with the early implementation (EI) of GAMMASPHERE [19] using the $^{54}\text{Fe}(^{58}\text{Ni},3p)$ reaction, with a 243-MeV ^{58}Ni beam provided by the 88 in. cyclotron at the Lawrence

Berkeley National Laboratory. Both thin- and backed-target experiments were performed. The thin target consisted of two self-supporting $500 \mu\text{g}/\text{cm}^2$ foils of 97% isotopically pure ^{54}Fe . At the time of the experiment, the GAMMASPHERE (EI) array consisted of 24 BGO-suppressed Ge detectors, each with an efficiency of approximately 75% relative to a standard 3×3 in.² NaI(Tl) crystal at 1.3 MeV. A forward-backward geometry with $\theta \leq 37^\circ$ or $\geq 143^\circ$ from the beam axis for the 24 Ge detectors minimized the effects of Doppler broadening; despite the large recoil velocity ($v/c=4.7\%$), the full width at half maximum (FWHM) of photopeaks at 1 MeV was measured to be ~ 6 keV after correcting for Doppler shifts. This geometry also favors detection of the stretched $E2$ transitions of the decoupled intruder bands because of their forward-backward peaked angular distributions resulting from the reaction-aligned residual nuclei. The backed target consisted of a $500 \mu\text{g}/\text{cm}^2$ ^{54}Fe foil backed with $15 \text{mg}/\text{cm}^2$ of Au.

Only events which satisfied a three-or-higher-fold suppressed-Ge coincidence trigger condition were accepted and written onto magnetic tape. Approximately 240×10^6 (thin target) and 80×10^6 (backed target) events were collected. Approximately 80% of the events were threefold and 20% were four-or-higher fold.

III. DATA ANALYSIS

The event data were analyzed with several different methods. First, they were unpacked into twofold coincidences and sorted into two-dimensional E_γ - E_γ matrices containing 880×10^6 (thin target) and 290×10^6 (backed target) doubles. Secondly, they were unpacked into threefold coincidences to form E_γ - E_γ - E_γ cubes, which contained 390×10^6 (thin target) and 100×10^6 (backed target) triples. The analysis method of using double-gated spectra extracted from the cubes proved to be essential for the determination of the complex level scheme of ^{109}Sb .

Thirdly, the data were unpacked into fourfold coincidences and sorted into several double-gated matrices with different gating conditions. In order to isolate weak coincidence cascades from contaminant contributions in a matrix, two gates were set on known low-lying γ energies in ^{109}Sb while sorting the two remaining coincident γ rays of a fourfold event. The combination of these double-gated matrices from the fourfold data and the double-gated spectra from the cube provided the sensitivity required for the study of high-spin intruder bands; this high sensitivity is also important in determining the weak terminating transitions and in investigating the elusive transitions linking the high-spin bands to the low-lying states of the nucleus.

Detailed analyses of the data in the cube and in the different matrices were performed with the analysis packages LEVIT8R (cube) and ESCL8R (matrix) [20]. With these programs, the γ transitions were arranged in the level scheme on the basis of coincidence relations, relative intensities, and γ -ray energy sums. The multipolarities of the γ transitions and the resulting spin-parity assignments of the energy levels are based on coincidence relationships, relative intensities, and known systematic structures in the neighboring nuclei. The directional correlation (DCO) results from the earlier ^{109}Sb experiment [7] provided important information in this

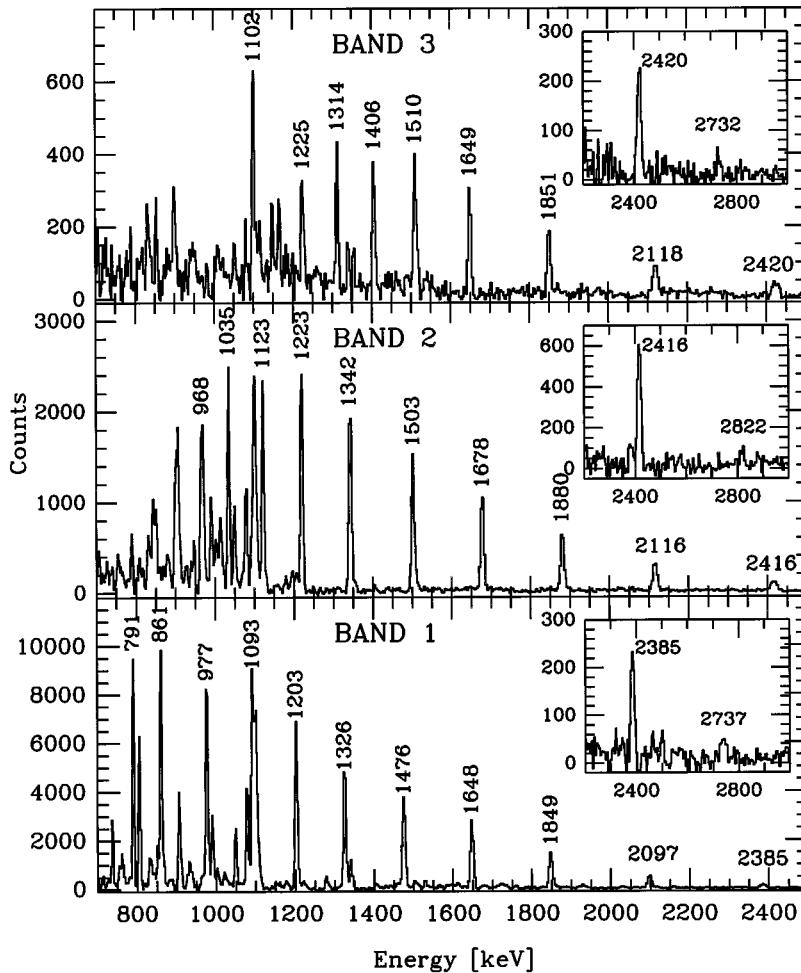


FIG. 1. Three coincidence γ -ray spectra for transitions in bands marked 1, 2, and 3 of ^{109}Sb . The spectra were created by summing double gated spectra from the GAMMASPHERE E_γ - E_γ - E_γ cube data. The spectra in the high-energy insets were obtained from a sum of single-gated γ -ray spectra from the doubles matrix to improve statistics, but this also introduced some additional contaminant bumps (note the small bump just below the 2416-keV peak in the inset for band 2, which does not appear in the double gated spectrum). Only peaks labeled satisfied the requisite double-gating conditions involving other transitions within the band; other peaks not labeled include coincident γ -ray transitions from the lower part of the level scheme (note the low-lying 1101-, 1106-, and 1111-keV transitions) or known strong contaminants from different reaction channels.

respect. Additional spin-parity information for ^{109}Sb below the intruder bands has recently become available [22]. For nonlinked intruder bands, minimum spins for the bands can be estimated from the spins of the levels into which they feed, plus allowances for the angular momentum of the linking transitions. Because the available valence configurations are simple for ^{109}Sb , being near a double shell closure, further spin information can be inferred from band termination spins and from the energy characteristics vs spin of the band, if the band configurations can be identified. Tentative spins for several nonlinked bands are based on such arguments (see Sec. V), but are consistent with the minimum spins implied from the experiment.

IV. EXPERIMENTAL RESULTS

The previous investigation of the ^{109}Sb nucleus by Janzen *et al.* [7] identified three $\Delta I = 2$ intruder bands. These bands were observed up to high rotational frequencies ($\hbar\omega \approx 1.4$ MeV) and showed gradually decreasing dynamic moments of inertia with increasing rotational frequency. The present study with GAMMASPHERE (EI) results in a substantial improvement in the γ -ray spectra for the bands at high energies and extends the spectroscopic information of the nucleus including two additional intruder bands.

Figure 1 shows double-gated γ -ray spectra obtained from the thin-target cube for the three previously reported intruder

bands in ^{109}Sb , marked 1–3. The spectra are sums of up to 64 clean gate combinations in each of the bands. The three spectra clearly show a gradual increase in the γ -ray energy spacings as the band γ -ray energies increase, implying a corresponding decrease in the dynamic moments of inertia. The spectra in the high-energy insets were obtained from a sum of single-gated γ -ray spectra from the doubles matrix; this had the desired effect of improving statistics in the high-energy peaks, but also introduced some additional contaminant bumps. Only peaks labeled in Fig. 1 satisfied the requisite double-gating conditions involving other transitions within the band. Other peaks not labeled include γ -ray transitions from the lower part of the level scheme following various feed-out paths for each band. With this information, all three bands were extended to higher spin with γ -ray transitions up to ~ 2.8 MeV. Remarkable for all the bands is the sharp drop in γ -ray intensity at the highest spin values with no further coincident transitions observed.

In addition, two new rotational bands, marked 4 and 5, were extracted from the data. The corresponding coincidence spectra are displayed in Fig. 2. Both of these bands were weakly populated in the reaction, each having an intensity less than 10% of the most intense transition in band 1. The peaks labeled in Fig. 2 satisfied the requisite double-gating conditions for bands 4 and 5. The inset for the high-energy transitions of band 4 was obtained as described above for bands 1–3. Transitions in band 4 were observed up to

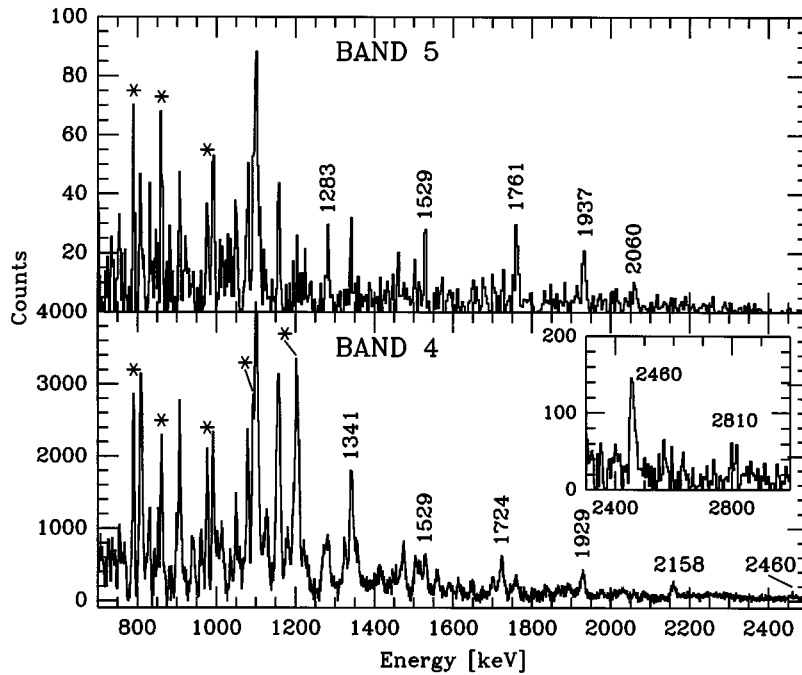


FIG. 2. Two coincidence γ -ray spectra for transitions in bands marked 4 and 5 of ^{109}Sb . The spectra were created by summing double gated spectra from the GAMMASPHERE E_{γ} - E_{γ} - E_{γ} cube data. The spectrum in the high-energy inset was obtained from a sum of single-gated γ -ray spectra from the doubles matrix to improve statistics, but this also introduced some additional contaminant bumps. Only peaks labeled satisfied the requisite double-gating conditions involving other transitions within the band; other peaks not labeled include coincident γ -ray transitions from the lower part of the level scheme (note the low-lying 1101-, 1106-, and 1111-keV transitions, which introduce a large unresolved coincident peak in both spectra) or known strong contaminants from different reaction channels. The peaks marked by an asterisk include coincident γ -ray transitions in band 1.

γ -ray energies of ~ 2.8 MeV, similar to bands 1–3, whereas in band 5 none were observed beyond 2.1 MeV. As can be seen in Fig. 2, the γ -ray energy spacings increase with increasing energy for band 4 following a pattern similar to bands 1–3; however, band 5 shows a decrease in the γ -ray spacings with increasing energy. The γ -ray transitions in bands 4 and 5 were found to be in coincidence with lower members of band 1, as indicated by asterisks in Fig. 2.

A partial level scheme of the high-spin region in ^{109}Sb , including all five $\Delta I = 2$ bands, is shown in Fig. 3. Despite the high quality of the data and good statistics for all of the bands, the feeding patterns into the known low-lying states of the nucleus were not completely identified. Thus only tentative spins and parities could be assigned to these band levels. The assigned spins for bands 1–5 represent estimates based first on lower spin limits for the decay-out members, obtained from states of known spin which were populated by the decay of each band and assuming unobserved linking γ -ray transitions. Secondly, the number of stretched $E2$ transitions observed in each band yields the range of spins between the highest band member and the feed-out member, and thus places a lower limit on the spin of the highest observed band member. In band 1, for example, a spin range of $24\hbar$ is observed from the twelve in-band transitions. Thirdly, the configurations calculated as yrast or close to yrast in this spin range are simple because of the proximity to the doubly closed shell and terminate at well-defined spin values compatible with the Pauli principle; the observed sharp drop in intensity for the highest transitions is consistent with band termination. With these three pieces of experimental information, that imply upper and lower spin limits together with the range of spins for these decoupled bands, there is considerable restriction on the possible spins of these ^{109}Sb intruder bands even when not directly linked to the lower part of the level scheme.

Theoretical calculations [1,2] in this closed shell region define band-energy characteristics and termination for available specific configurations over the observed spin range; the

calculations have been successfully applied to a number of linked bands in this region where the spins are known (^{108}Sn , $^{110,111,113}\text{Sb}$, ^{114}Te) [2,10,21], and to the nonlinked bands 1–3 of ^{109}Sb [1] from this experiment. Therefore, the above experimental information has been applied with the guidance of these calculations to make the tentative spin assignments shown in Fig. 3. These assignments are used in discussing the experimental band properties in this section, but the detailed arguments for the specific configurations are given in Sec. V.

For band 1, which is the most intense, a number of transitions involved in the decay were identified prior to the unobserved linking transitions. To extract these results, four-fold events were used by sorting different combinations of double-gated matrices. Several parallel decay branches are observed in the decay pattern, which reduces the intensity of each individual branch and limits further identification of the γ rays involved in the coincidence spectra. The majority of the decay-out of band 1 occurs at the $(35/2^-)$ level, where at least five competing decay branches are involved as shown in Fig. 3. The sequence including the 806–738 keV γ -ray transitions was found to have the strongest intensity. A significant part of the intensity is further taken away by the 593 keV γ -ray transition, in addition to the 622–762 keV decay sequence out of the $(39/2^-)$ level, which is placed parallel to the 791 keV γ -ray transition.

Although bands 4 and 5 both feed into the lower levels of band 1, it was not possible to identify the linking γ -ray transitions involved. Minimum spins for these two bands can be estimated from the tentative spins of the levels in band 1 into which they feed, plus allowances for the angular momentum of the linking transitions. Band 4 is found to feed into the $(55/2^-)$ level of band 1, whereas band 5 feeds into the lower $(47/2^-)$ level, which indicates a lower excitation energy of band 5 compared to band 4. Coincidences with band-1 transitions are marked by asterisks in Fig. 2; the large peak near 1100 keV includes several coincident γ rays (1101, 1106, and 1111 keV) from the lower part of the level scheme.

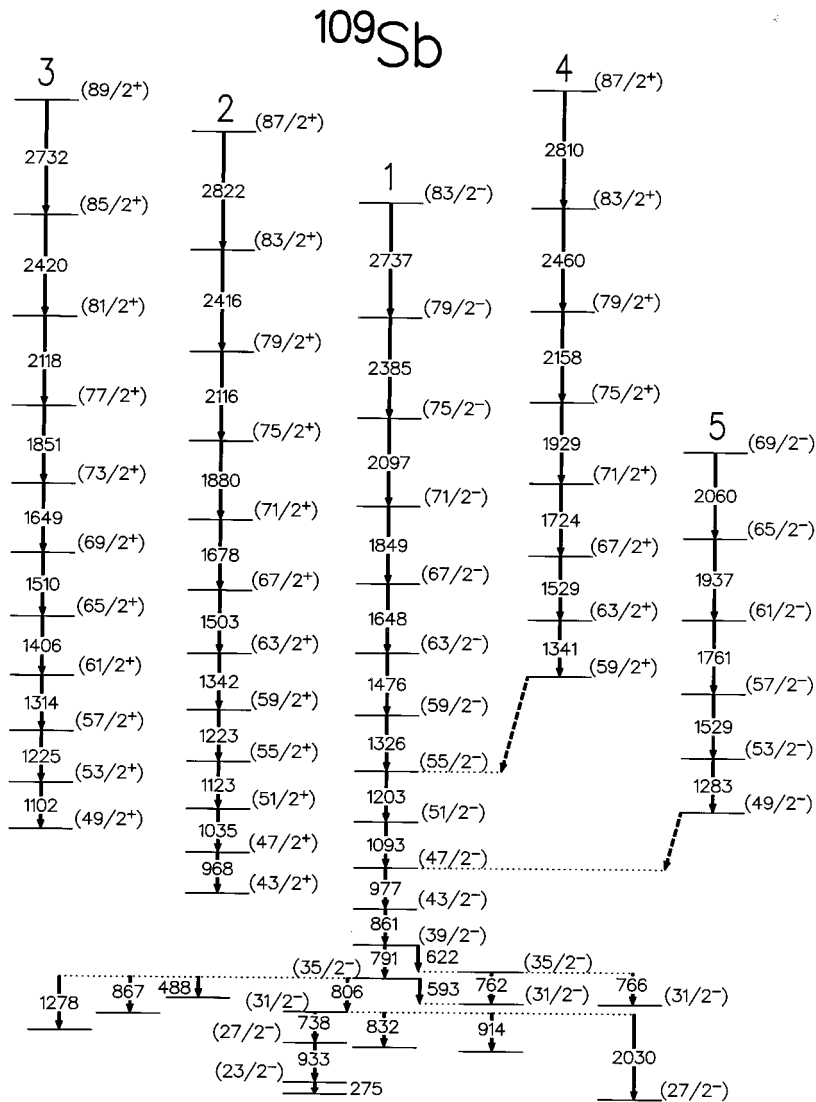


FIG. 3. A partial level scheme which includes all five decoupled bands 1–5 observed in ^{109}Sb . Gamma ray energies are given in keV.

In addition to the large number of irregular single-particle levels at low excitation energies, two strongly coupled bands (bands 6 and 7) were observed in this nucleus as shown in Fig. 4. A typical double-gated coincidence spectrum from the cube, shown in Fig. 5, reveals the transitions in band 6; the 417/462 keV double gate discriminates against the side-band that feeds into band 6 (see Fig. 4). The strongly coupled bands appear as sequences of very intense $\Delta I=1$ transitions and weak $\Delta I=2$ crossover transitions. These bands further extend the systematics of similar structures observed in the heavier Sb nuclei. Band 6 favors decay into positive-parity states, and thus is believed to have positive parity, consistent with extensive systematics; the majority of the decay is observed to populate the $15/2^+$ and $17/2^+$ spherical levels. Band 7, at a higher excitation energy, is tentatively assigned negative parity because it decays predominantly into the yrast $19/2^-$ state with two parallel decay γ -ray sequences of similar energy, 241–758 keV and 243–756 keV. Angular distribution and linear polarization results [22] implied stretched $M1$ transitions for these sequences.

The level scheme presented in Fig. 4 also shows the states which are populated by the decay of the high-spin intruder $\Delta I=2$ bands. These results were obtained by comparing the

intensities in different threefold and fourfold spectra, where gates were chosen to be within an intruder band and another gate placed on a γ -ray peak in the low-spin part of the level scheme, to isolate the levels of interest. Band 1 was found to populate almost every negative-parity level above spin $15/2$, and thus is assumed to be of negative parity. The most intense feeding is into the negative-parity bandlike sequence shown between bands 6 and 7 in Fig. 4; the 844-843 (doublet), 1050, 554, and 180 keV γ rays coincident with band 1 indicated this feeding into the $23/2^-$ up to the $31/2^-$ or $35/2^-$ levels of this sequence. Bands 2 and 3 are less intense, and only an indication of feeding into a $35/2^-$ state could be identified, as shown.

V. DISCUSSION

The nuclear structure of the $Z=51$ ^{109}Sb nucleus can be classified in terms of the number of proton particle-hole (p-h) excitations across the $Z=50$ closed shell involved in the specific configurations. The $0p-0h$ states are simply those states formed by the valence proton occupying the low lying $\pi d_{5/2}$, $\pi g_{7/2}$, or $\pi h_{11/2}$ orbitals (the $\pi d_{5/2}$ and $\pi g_{7/2}$ orbitals are nearly degenerate) coupled to the $Z=50$ ^{108}Sn near-

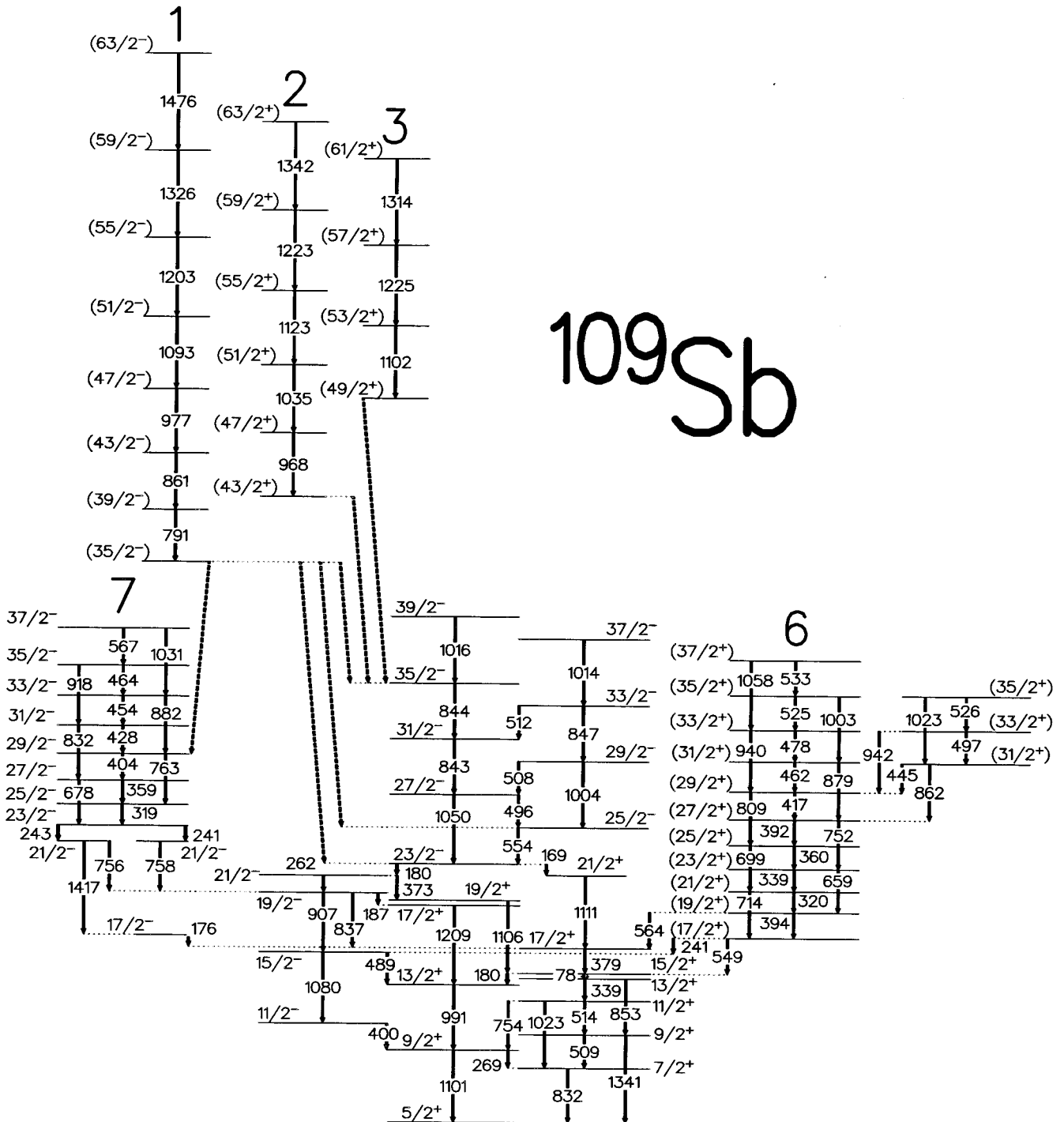


FIG. 4. Low energy part of the ^{109}Sb level scheme which shows the observed complex spherical states as well as two strongly coupled bands. Indications of the feeding patterns for the intruder bands are also shown. γ -ray energies are given in keV.

spherical core, e.g., the $0^+ - 2^+ - 4^+$ ground-state sequence [8] with energy spacings 1206 and 905 keV. The corresponding ^{109}Sb $5/2^+ - 9/2^+ - 13/2^+$ sequence with 1101 and 991 keV spacings, and $11/2^- - 15/2^- - 19/2^-$ sequence with 1080 and 907 keV spacings as shown in Fig. 4 are readily identifiable with the $\pi d_{5/2}$ and $\pi h_{11/2}$ orbitals, respectively. The $7/2^+ 0^+ \otimes \pi g_{7/2}$ state can be seen at 832 keV above the ground state. These features are consistent with the earlier ^{109}Sb experiments [7,22]. Spherical negative-parity core states

($7^-, 9^-$) involving the $\nu h_{11/2}$ orbital in ^{108}Sn can couple to the same valence proton orbitals; although such spherical states have been observed in ^{111}Sb [12], they are not easily identified in ^{109}Sb .

The 1p-1h proton excitations across the $Z=50$ gap are involved, for example, in the low-lying $2p1h \pi(g_{7/2}d_{5/2})(g_{9/2})^{-1}$ configuration in ^{109}Sb ; this deformed proton configuration is manifest in bands 6 and 7 that are shown in Fig. 4. The 2p-2h proton excitations appear lowest

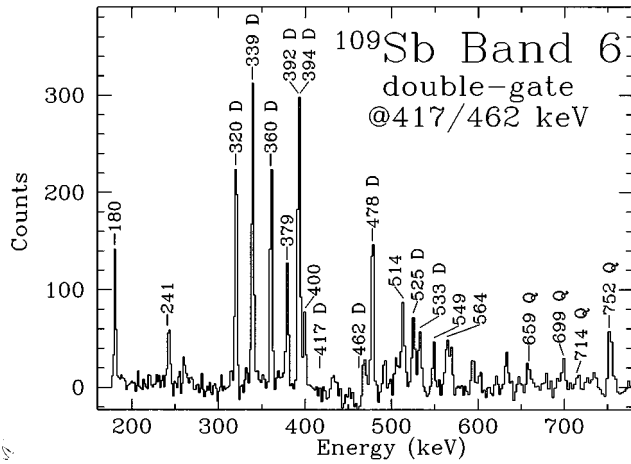


FIG. 5. A typical double-gated γ -ray spectrum from the cube for the 417/462 keV transitions in the strongly coupled band 6 of ^{109}Sb . The gates were chosen to discriminate against the sideband that feeds into band 6. The lines labeled “D” are the predominantly $M1$ -dipole $\Delta I=1$ transitions while those labeled “Q” are the $E2$ -quadrupole crossover transitions.

in ^{109}Sb as a coupling of the $\pi[(g_{7/2}d_{5/2})^2(g_{9/2})^{-2}]$ deformed core configuration of ^{108}Sn to the deformation driving valence $\pi h_{11/2}$ proton orbital, namely a $3p2h$ configuration. Bands 1–3, shown in Fig. 3, involve this deformed proton configuration. The observed rotational bands interpreted in terms of these types of deformed states, along with additional aligned particles outside of the $Z=N=50$ doubly closed core, will be discussed in separate sections below. The focus of this work is the experimental investigation of these intruder bands, particularly those related to the $2p-2h$

proton excitations across the $Z=50$ shell gap, and their interpretation in terms of the smooth band termination [1].

Our calculations [1], which utilized a configuration-dependent shell-correction approach with cranking, were performed to investigate and identify the configurations in ^{109}Sb involved in the intruder bands as well as to understand the band termination properties. A recent application of these calculations to the $A=110$ region investigates the details of the predicted nuclear structure features [2]. A Nilsson-Strutinsky cranking method [23], involving a modified oscillator model along with specific techniques [1,2] for identifying the $N=4$ $g_{9/2}$ proton holes and the particles in other $N=4$ subshells ($g_{7/2}, d_{5/2}, \dots$), has been employed. The calculations minimize the energy with respect to the deformation parameters ($\epsilon_2, \epsilon_4, \gamma$). Since pairing correlations have been neglected, the theory does not address the alignment features at low frequencies, $\hbar\omega \leq 0.7$ MeV. An important property for ^{109}Sb is that an intruder band related to a specific configuration without admixtures can be followed over a large spin range to the maximum spin allowed by the configuration at band termination. Calculated $E-E_{\text{LD}}$ for bands based on $0p-0h$, $1p-1h$, $2p-2h$, and $3p-3h$ proton excitations across the $Z=50$ gap are displayed in Fig. 6 for the four combinations of parity π and signature α , where the rotational liquid drop energy $E_{\text{LD}} = (\hbar^2/2\mathcal{J}_{\text{rig}})I(I+1)$. The configuration notation used follows that of Ref. [2], where $[p_1p_2, n]$ are the numbers of proton holes in the $g_{9/2}$ orbital, of protons in the $h_{11/2}$ orbital, and of neutrons in the $h_{11/2}$ orbital, respectively. The observed bands in ^{109}Sb will be compared to these calculations for specific band configurations in Fig. 7 and discussed in the following sections. The smooth band termination feature and related nuclear shape changes will be discussed in the last section.

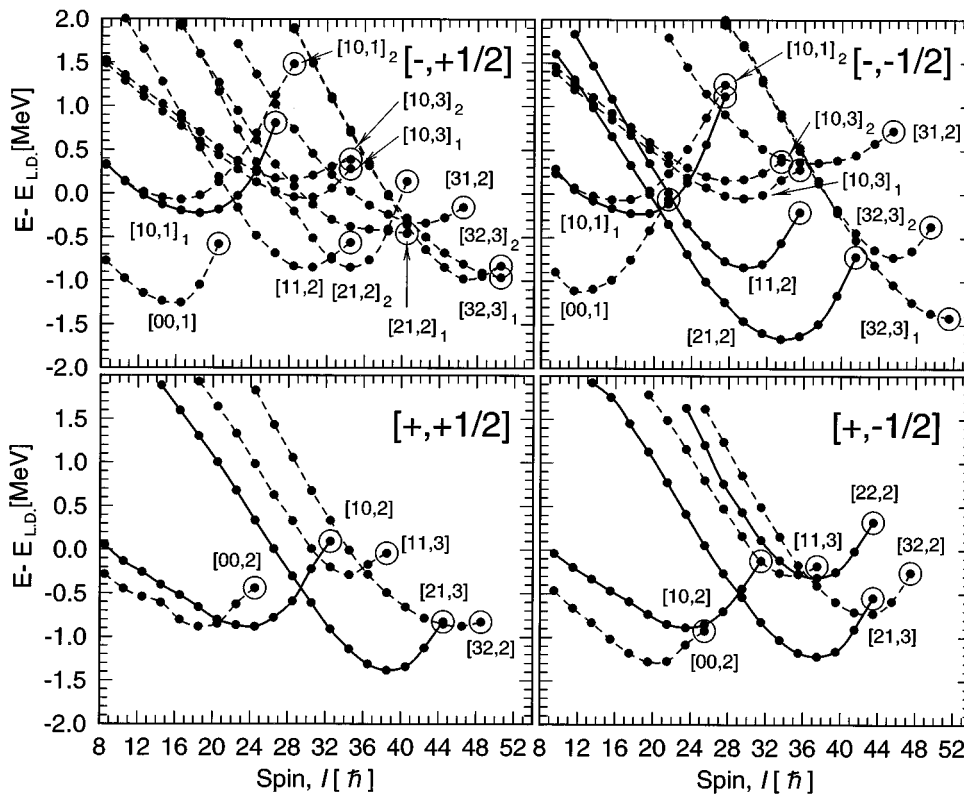


FIG. 6. $E-E_{\text{LD}}$ calculations for the four combinations of parity and signature, $[\pi, \alpha]$, for band configurations in the yrast region of ^{109}Sb , where $E_{\text{LD}} = (\hbar^2/2\mathcal{J}_{\text{rig}})I(I+1)$ with $\hbar^2/2\mathcal{J}_{\text{rig}} = 0.013$ MeV. The configuration notation used is $[p_1p_2, n]$, where p_1 is the number of proton holes in the $g_{9/2}$ orbital, p_2 is the number of $h_{11/2}$ protons, and n is the number of $h_{11/2}$ neutrons. The subscripts used with this notation are for the cases where the same $[p_1p_2, n]$ are obtained as a consequence of different distributions of particles (holes) with signature $\alpha = -1/2$ and $\alpha = +1/2$. The large open circles indicate band termination states for the specific configurations. Full lines are used for configurations assigned to the observed bands 1–7 (see Fig. 7), while other (unobserved) configurations are shown by dashed lines.

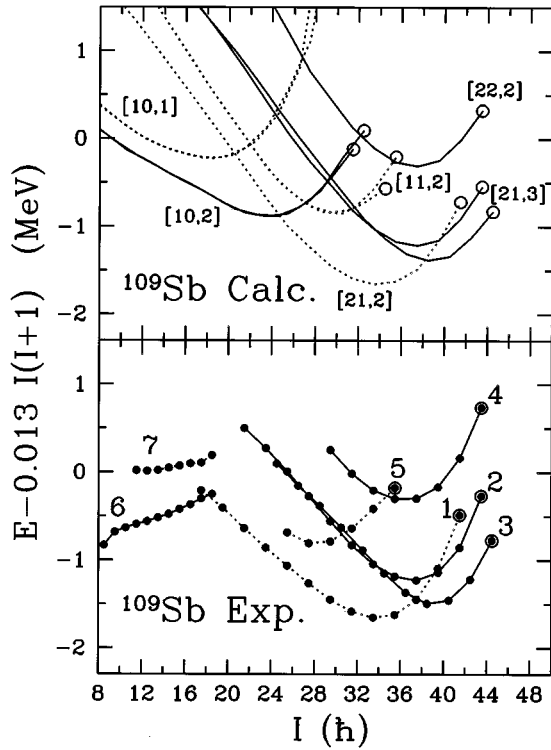


FIG. 7. Comparison as a function of spin between calculated and observed $E-E_{LD}$ for the identified intruder band configurations in ^{109}Sb . The circles indicate band termination states. The experimental energy scales are relative for the nonlinked intruder bands.

A. Intruder bands involving 2p-2h proton excitations

1. Intruder bands 1-3

The intruder bands 1-3 shown in Fig. 3 were those first discovered by Janzen *et al.* [7]. The improved sensitivity of the GAMMASPHERE (EI) array allowed the extraction of the transitions at the top of these bands with γ -ray energies near 2.8 MeV, representing very high rotational frequencies. In addition, the observed significant drop in intensity for the last transition in each of these bands, as documented in Fig. 1, is consistent with band termination. Although substantially more information was obtained regarding the feeding patterns of these bands to the known lower energy portion of the level scheme, definite links were not established. As discussed in Sec. IV, the spin assignments for the bands shown are thus tentative; however, using lower spin limits from the band feed-out transitions, spin ranges of the bands, and termination spins for the available configurations, the band spins have considerable definition. Further guidance was achieved from theoretical calculations [1,2] for the configurations in ^{109}Sb , which are yrast or close to yrast in the spin range $I \sim 30-45\hbar$. The spins and parities listed for the band members are consistent with those selected for the band-termination interpretation (see Figs. 6 and 7). The energy characteristics of the bands as a function of spin, as shown by these $E-E_{LD}$ curves, provide additional information about the available configurations and thus the spin, independent of the termination spin. In particular, each of the curves reveals a minimum as a function of spin, which results from the transition within the band from high collectivity to a non-

collective terminating state. The agreement of the spins at which the calculated minima and the experimental minima occur represents a confirmation of the configuration. This agreement is observed for the linked yrast [20,2] band in ^{108}Sn , which is directly related to the [21,2] configuration identified with band 1 in ^{109}Sb .

Applying the spin arguments discussed above, band 1 decaying out at $(35/2^-)$ and terminating at $(83/2^-)$, just fits its $24\hbar$ spin range between the lower and upper spin limits of the observed decay-out and the termination spin of the [21,2] configuration. Bands 2 and 3 terminating at $(87/2^+, 89/2^+)$, respectively, consistent with the [21,3] signature partners, then decay out at higher spins as shown; this leaves an angular momentum gap between the bottom of the bands 2 and 3 and the observed lower limit ($4\hbar$ for band 2, the $-1/2$ signature component), which is not unreasonable in view of the change in parity required for this configuration. Detailed arguments for these two configurations are given below. The dynamic moments of inertia $\mathcal{J}^{(2)}$ for bands 1-3 are plotted in Fig. 8; they show the characteristic smooth decrease with increasing spin or frequency to unusually low values, near $1/3$ the rigid-body value, at frequencies near $1.4 \text{ MeV}/\hbar$.

The structure of band 1, which appears to be yrast over a large spin region, is expected to involve the low- Ω $h_{11/2}$ proton coupled to the 2p-2h proton excitations of the ^{108}Sn core. The deformed $[\pi(g_{7/2}d_{5/2})^2(g_{9/2})^{-2}]$ configuration is the basis of low lying positive-parity rotational bands observed in the even Sn nuclei from ^{108}Sn to ^{118}Sn [4,8]. This feature, where the valence $h_{11/2}$ proton is coupled to both spherical and deformed core states, has been observed previously in several odd-A Sb isotopes [5,6,12]. The bands, corresponding to the deformed 2p2h core, systematically begin to decay out near the $23/2^-$ member into states where the valence $h_{11/2}$ proton is coupled to the spherical 4^+ core state, as was the case for $^{111,113}\text{Sb}$. In ^{109}Sb , band 1 decays out somewhat higher in spin, near $35/2^-$, consistent with the higher excitation energy for the 2p2h deformed band in the ^{108}Sn core. It is thus expected that band 1 in ^{109}Sb initiates from the deformed $\pi h_{11/2}[(g_{7/2}d_{5/2})^2(g_{9/2})^{-2}]$ proton configuration. The theoretical calculations (see Fig. 6) show that this proton configuration is responsible for the lowest lying structure in this spin range. At the highest spins, the complete configuration [21,2] with respect to the $Z=N=50$ doubly closed shell is $\pi h_{11/2}[(g_{7/2}d_{5/2})^2(g_{9/2})^{-2}] \otimes \nu(g_{7/2}d_{5/2})^6(h_{11/2})^2$. As shown in Fig. 6, this band terminates at $83/2^-$. The experimental band energies presented in the same manner, namely relative to the rotating liquid drop values, are shown in the lower part of Fig. 7 for the assigned spins; the corresponding calculated [21,2] result is displayed in the upper part of the same figure for comparison purposes. The comparison of the experimental and calculated curves for band 1 shows a remarkable agreement in shape with both the experimental- and the theoretical-curve minima occurring at $67/2 \hbar$, which adds confirmation to these assignments.

The most favorable interpretation for bands 2 and 3 involves the promotion from the band-1 configuration of a neutron from the $(g_{7/2}d_{5/2})$ orbital to the $h_{11/2}$ orbital giving positive parity; the two curves labeled [21,3] in Fig. 6 represent this interpretation. The two bands would be the two

signature partners of this configuration, where the high- Ω positive-parity neutron orbital implies a small signature splitting. This favored [21,3] configuration, which for bands 2 and 3 would include the same proton configuration as for band 1 but with three $\nu h_{11/2}$ neutrons is $\pi h_{11/2}[(g_{7/2}d_{5/2})^2(g_{9/2})^{-2}] \otimes \nu(g_{7/2}d_{5/2})^5(h_{11/2})^3$. The two bands representing the [21,3] signature partners, shown in Fig. 6, terminate at spins $87/2^+$ and $89/2^+$. Again the comparisons in Fig. 7 between the [21,3] calculations and the experimental results for bands 2 and 3 are excellent in regard to the shapes of the curves, with the minima occurring at $75/2$ and $77/2 \hbar$, respectively, for the two signatures. Bands associated with this [21,3] configuration in ^{110}Sb and in ^{111}Sb show similar agreement with the calculations (see Refs. [2,21]); the spins are known for the ^{110}Sb band as it is linked.

2. Band 4

As indicated in Fig. 3, seven transitions were extracted for band 4 with the top transition having an energy of 2810 keV. The band is observed to feed into band 1 at the $(55/2^-)$ level with significant intensity, although the connecting links are not established. This feeding suggests high spins and higher excitation energies for band 4. Following an examination of the cranking calculations shown in Fig. 6, the band configuration that best satisfies the experimental characteristics of band 4 is the [22,2] configuration, which involves the promotion of one proton from the 2p2h deformed core to the next available $h_{11/2}$ orbital; excited bands based on the corresponding [21,2] configuration in ^{108}Sn have been observed [8]. Only one signature for the [22,2] configuration is shown in Fig. 6 because of the large signature splitting caused by the proton in the low- Ω positive-parity orbital; this is consistent with experiment, where only one signature (band 4) was observed. The complete configuration is $\pi(g_{7/2}d_{5/2})(h_{11/2})^2(g_{9/2})^{-2} \otimes \nu(g_{7/2}d_{5/2})^6(h_{11/2})^2$ having a termination spin of $87/2^+$. The comparison of the experimental and calculated energies in Fig. 7 shows that band 4 is in good agreement with the detailed characteristics of the curve representing the [22,2] configuration with the minimum occurring near $75/2 \hbar$. The dynamic moments of inertia ($\mathcal{J}^{(2)}$) for band 4 shown in Fig. 8 reveal the characteristic smooth decrease with increasing frequency to low values consistent with the intruder bands 1–3.

B. Deformed structure involving 1p-1h proton excitations

1. Band 6—positive parity $\Delta I=1$ band

The 2p1h bands based on the $\pi(g_{7/2}d_{5/2})^2(g_{9/2})^{-1}$ configuration have been observed [3,12] in odd-A Sb nuclei for neutron numbers $N=60-72$ with the minimum in excitation energy occurring near $N=68$. The crossing of the $\pi g_{7/2}$ and $\pi g_{9/2}$ orbitals at a prolate deformation results in more modest deformations for these 1p-1h excitations than for the 2p-2h proton excitations discussed in the previous section. The high- Ω $\pi g_{9/2}$ hole orbital implies there is no signature splitting for the resulting $9/2^+$ $\Delta I=1$ bands in agreement with experiment. For ^{111}Sb at $N=60$, this proton 2p1h strongly coupled band is the first case observed not to decay down to the $9/2^+$ bandhead, but instead decays out at the

$I^\pi=21/2^+$ member [12]. This change in the decay process has been attributed to a decrease in deformation of the $\pi(g_{7/2}d_{5/2})^2(g_{9/2})^{-1}$ bandhead as N decreases below $N=68$. The corresponding $\Delta I=1$ band observed in ^{109}Sb is shown on the right (band 6) of Fig. 4. The $\Delta I=1$ in-band transitions of the band are observed up to $I^\pi=(37/2^+)$ along with weaker $E2$ crossovers, the intensity ratios of which are consistent with the high K value. This band decays out at the $I^\pi=(19/2^+)$ and $(17/2^+)$ members; these branches are not completely determined because of the low individual-branch intensities and the complex coincidence spectra, making the spins tentative. A sideband of three levels was observed to feed into band 6 as shown in Fig. 4.

The present calculations shown in Fig. 7 include this 2p1h band, labeled [10,2], which has the complete configuration relative to $Z=N=50$ of $\pi(g_{7/2}d_{5/2})^2(g_{9/2})^{-1} \otimes \nu(g_{7/2}d_{5/2})^6(h_{11/2})^2$. The [10,2] band configuration has nonyrast terminating states with spins of $63/2^+$ and $65/2^+$, respectively, for the two signatures. Note that since pairing is not included, the calculations are not expected to reproduce the experimental curves below $20\hbar$. In addition, the experiment does not follow this positive parity band 6 to near the predicted termination spins. Nonetheless, the calculations for these configurations are included in Fig. 7 for completeness. The tentative $I^\pi=(37/2^+)$ band member reached in the present experiment involves two band transitions beyond that reported in Ref. [22]. None of these odd-A Sb 2p1h bands have been seen to high spins; in ^{111}Sb , this related band was followed only up to $41/2^+$ [12].

The fact that these bands with 1p-1h proton excitations have only modest deformations might be the reason that they are not followed experimentally up to spins near termination. One should note that these collective structures of low deformation reveal similarities with the so-called ‘‘shears bands’’ which characteristically show γ -ray intensities that fall off at spins limited by the allowed tilted-axis alignment. Indeed, these structures in ^{109}Sb are based on the high- Ω proton hole ($\pi g_{9/2}$) and the low- Ω neutrons ($\nu h_{11/2}$). This is analogous to structures in the Pb nuclei where the ‘‘shears bands’’ according to the tilted-axis cranking interpretation [24] are formed by low- Ω proton particle states ($h_{9/2}$ and $i_{13/2}$) and high- Ω neutron hole states ($i_{13/2}$).

2. Band 7—negative parity $\Delta I=1$ band

Band 7, shown in Fig. 4, is a second $\Delta I=1$ band with properties very similar to those of band 6, namely strong $\Delta I=1$ transitions with weak $E2$ crossover transitions, and no signature splitting. Negative-parity $\Delta I=1$ bands have been previously reported [12] in other odd-A Sb isotopes. They have been interpreted as based on the $\pi(g_{7/2}d_{5/2})^2(g_{9/2})^{-1} \otimes J^-$ configuration, where J^- refers to a two-neutron state ($7^-, 5^-$) of the Sn core nucleus involving one $\nu h_{11/2}$ orbital and one positive-parity orbital. This interpretation is consistent with several measured electromagnetic properties including a sensitive time-differential magnetic-moment measurement in ^{117}Sb [25]. Band 7, which decays out at a $23/2^-$ state and is observed up to the $37/2^-$ member, is believed to be related to this configuration. The present calculations for the configuration [10,1] involving one $h_{11/2}$ neutron do not follow the experimental curve for band 7. The

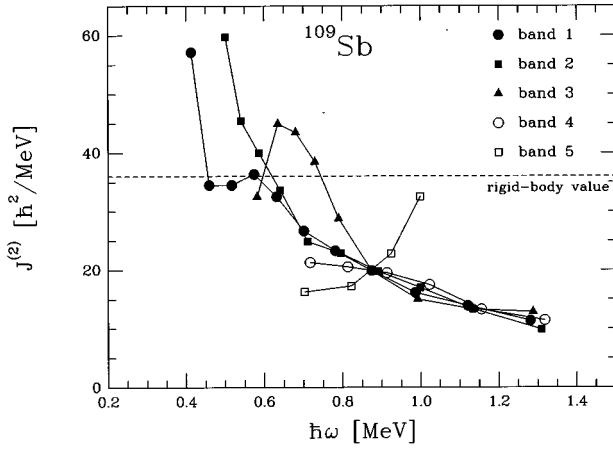


FIG. 8. Observed dynamic moments of inertia, $\mathcal{J}^{(2)}$, as a function of frequency for the five intruder bands 1–5.

calculations show this band to become nonyrast at the higher spins as shown in Fig. 7, and predict that the two signature branches would not terminate until $57/2^-$ and $59/2^-$, respectively. The $[10,3]$ configuration with three $\nu h_{11/2}$ orbitals has a higher excitation energy at these low spins, as shown in Fig. 6.

3. Band 5

Only five transitions were extracted for band 5, which was relatively weakly populated. It was observed to feed into the $(47/2^-)$ member of band 1, which implies a lower spin limit for the top member of $(69/2^-)$, assuming an unobserved stretched dipole linking transition. The calculations shown in Fig. 6 for this spin range suggest the configuration $[11,2]$, namely $\pi(g_{7/2}d_{5/2})(h_{11/2})(g_{9/2})^{-1} \otimes \nu(g_{7/2}d_{5/2})^6(h_{11/2})^2$, involving 1p-1h proton excitation, for which the two signatures terminate at $69/2^-$ and $71/2^-$. If the unobserved linking transition were a stretched quadrupole, band 5 would be consistent with the other signature and a termination spin of $71/2^-$. The fact that band 5 with a 1p-1h core excitation is followed to termination, where bands 6 and 7 are not, could be explained by the extra deformation-driving property of the $h_{11/2}$ proton. The experimental and calculated energy comparison as a function of spin in Fig. 7 shows that band 5 agrees well with either signature of this $[11,2]$ configuration, although the fact that only one signature was observed causes some doubt about this assignment. The $\mathcal{J}^{(2)}$ for band 5 plotted in Fig. 8 shows a significant change from the other intruder bands; rather than decreasing with increasing frequency, the $\mathcal{J}^{(2)}$ increases sharply. This feature is not understood, but the rise of $\mathcal{J}^{(2)}$ is only seen at two frequency points and could thus be caused by small disturbances of the transition energies, e.g., from some band mixing. In this sense, the energy comparison in Fig. 7 appears to be a better test of the configuration than the $\mathcal{J}^{(2)}$ comparison.

C. Smooth-band termination

Theoretical calculations [1] were undertaken to interpret the intruder bands observed in ^{109}Sb which showed the characteristic features of decreasing dynamic moments of inertia

up to very high frequencies, and termination spins consistent with the aligned spins for the valence particles and holes relative to the $Z=N=50$ doubly closed core. Because of the fact that specific configurations could be followed over a large spin range, theoretical and experimental comparisons, as shown in Fig. 7, were highly successful for the band-member energies as a function of spin without the difficulties of significant admixtures with other bands. The calculated dynamic moments of inertia $\mathcal{J}^{(2)}$ for the assigned band configurations (bands 1–6) are displayed as a function of frequency in Fig. 9. A smoothing technique has been applied to these $\mathcal{J}^{(2)}$ curves to avoid fluctuations from a second derivative of energy versus spin, as discussed in Ref. [1]; the large solid circles in Fig. 9 show the unsmoothed calculation for band 1. These calculations agree well with the experimental $\mathcal{J}^{(2)}$ values for the intruder bands 1–4 shown in Fig. 8 and thus explain the strongly increasing band spacings with increasing spin. The theory does not reproduce the observed rise in $\mathcal{J}^{(2)}$ for band 5, which, being well above yrast, may be subject to mixing.

The change in the intrinsic nuclear shape of the intruder bands as a function of spin can be seen by the calculated trajectories [1,2] for five of these bands in the (ϵ_2, γ) plane for various spins, as shown in Fig. 10. The configurations of the bands involve p-h excitations across the $Z=50$ shell gap, which result in prolate ($\gamma=0^\circ$) shapes at moderate spins because of the $\pi g_{7/2} - \pi g_{9/2}$ level crossing at $\epsilon_2 \approx 0.2$. The bands thus initially involve collective rotation about an axis perpendicular to the symmetry axis. As the rotational frequency increases, the Coriolis interaction initiates the alignment of the valence-particle spins which causes the nuclear shape to gradually trace a path through the triaxial (γ) plane, as shown, toward the noncollective single-particle shape at $\gamma=+60^\circ$. After the aligned valence-particle spin is exhausted, consistent with the Pauli principle, the band terminates. The calculated termination spins for the specific configurations, which are consistent with the experimental results, are shown in Fig. 7. This gradual change from collective prolate ($\gamma=0^\circ$) to noncollective oblate ($\gamma=+60^\circ$)

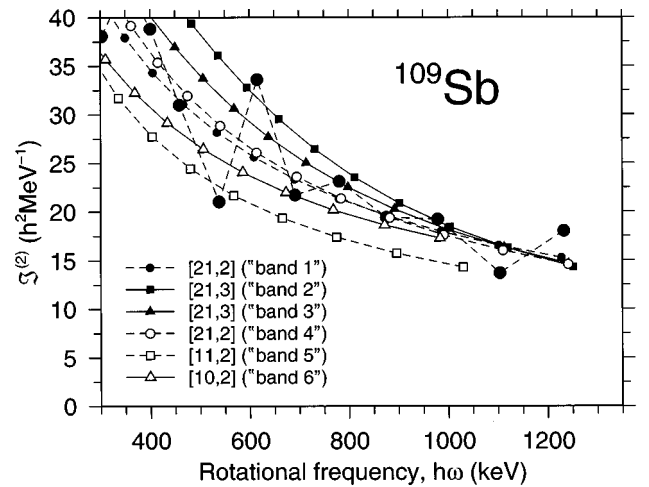


FIG. 9. Calculated dynamic moments of inertia $\mathcal{J}^{(2)}$ as a function of frequency for the intruder bands. Small symbols represent smoothed calculations; large circles represent unsmoothed band-1 calculations. See text regarding calculation details.

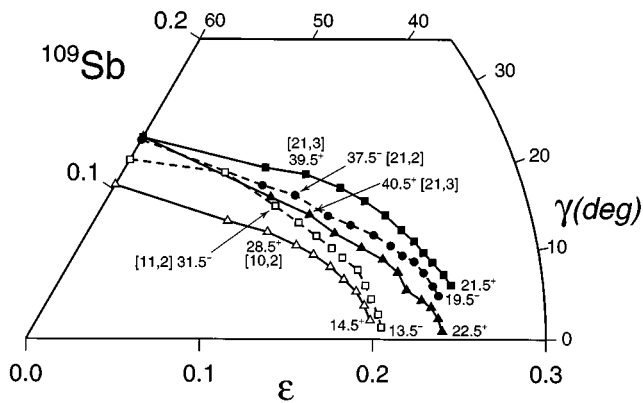


FIG. 10. Plot of the intrinsic nuclear shape calculated as a function of spin for five of the intruder bands in ^{109}Sb . The band identification symbols are the same as in the previous figure.

is accompanied by a smooth increase in the γ -ray energy spacings and a corresponding decrease in the dynamic moment of inertia leading to the so-called smooth-band termination. The intruder bands observed in the heavier odd- A Sb isotopes appear not to have reached termination spins, which are generally predicted to have higher values because of the additional valence particles available.

VI. CONCLUSIONS

Intruder rotational bands in ^{109}Sb have been investigated with GAMMASPHERE (EI) to high frequency. A total of seven collective structures involving proton particle-hole excitations across the $Z=50$ closed shell gap were observed to coexist with the normal single-particle structure. Four of the $\Delta I=2$ intruder bands, which are interpreted as being based on $2p$ - $2h$ proton excitations, reached tentative termination spins associated with the spin alignment of all the valence nucleons outside of ^{100}Sn . The band energies and decreasing dynamic moments of inertia as a function of spin are in good agreement with smooth band termination calculations. Two observed $\Delta I=1$ bands involving $1p$ - $1h$ proton excitations have properties consistent with a $\pi g_{9/2}$ hole in the $Z=50$ closed shell.

ACKNOWLEDGMENTS

This work was supported in part by the U.S. National Science Foundation, UK EPSRC, NATO (Grant No. CRG 910182), AECL, the Canadian NSERC, the Swedish Natural Science Research Council, and the Crafoord Foundation (Lund, Sweden). K.H. acknowledges receipt of financial support from the University of York. We also wish to thank the staff of the LBNL (GAMMASPHERE) facility.

- [1] I. Ragnarsson, V.P. Janzen, D.B. Fossan, N.C. Schmeing, and R. Wadsworth, *Phys. Rev. Lett.* **74**, 3935 (1995).
- [2] A.V. Afanasjev and I. Ragnarsson, *Nucl. Phys.* **A591**, 387 (1995).
- [3] A.K. Gaigalas, R.E. Shroy, G. Schatz, and D.B. Fossan, *Phys. Rev. Lett.* **35**, 555 (1975); *Phys. Rev. C* **19**, 1324 (1979).
- [4] J. Bron, W.H.A. Hesselink, A. Van Poelgeest, J.J.A. Zalmstra, M.J. Uitzinger, H. Verheul, K. Heyde, M. Waroquier, H. Vincx, and P. Van Isacker, *Nucl. Phys.* **A318**, 335 (1979).
- [5] D.R. LaFosse, D.B. Fossan, J.R. Hughes, Y. Liang, P. Vaska, M.P. Waring, and J.-y. Zhang, *Phys. Rev. Lett.* **69**, 1332 (1992).
- [6] V.P. Janzen, H.R. Andrews, B. Haas, D.C. Radford, D. Ward, A. Omar, D. Prévost, M. Sawicki, P. Unrau, J.C. Waddington, T.E. Drake, A. Galindo-Uribarri, and R. Wyss, *Phys. Rev. Lett.* **70**, 1065 (1993).
- [7] V.P. Janzen, D.R. LaFosse, H. Schnare, D.B. Fossan, A. Galindo-Uribarri, J.R. Hughes, S.M. Mullins, E.S. Paul, L. Persson, S. Pilotte, D.C. Radford, I. Ragnarsson, P. Vaska, J.C. Waddington, R. Wadsworth, D. Ward, J. Wilson, and R. Wyss, *Phys. Rev. Lett.* **72**, 1160 (1994).
- [8] R. Wadsworth, H.R. Andrews, R.M. Clark, D.B. Fossan, A. Galindo-Uribarri, J.R. Hughes, V.P. Janzen, D.R. LaFosse, S.M. Mullins, E.S. Paul, D.C. Radford, H. Schnare, P. Vaska, D. Ward, J.N. Wilson, and R. Wyss, *Nucl. Phys.* **A559**, 461 (1993).
- [9] D.B. Fossan, D.R. LaFosse, H. Schnare, C.W. Beausang, K. Hauschild, I.M. Hibbert, J.R. Hughes, V.P. Janzen, S.M. Mullins, E.S. Paul, D.C. Radford, I. Ragnarsson, I. Thorslund, P. Vaska, R. Wadsworth, and M.P. Waring, in *Proceedings of the Conference on Physics from Large γ -Ray Detector Arrays*, Berkeley, 1994 (Lawrence Berkeley Laboratory, Berkeley, 1994), Vol. 2, p. 194.
- [10] R. Wadsworth, C.W. Beausang, M. Cromaz, J. DeGraaf, D.B. Fossan, S. Flibotte, A. Galindo-Uribarri, K. Hauschild, I.M. Hibbert, G. Hackman, J.R. Hughes, V.P. Janzen, D.R. LaFosse, S.M. Mullins, E.S. Paul, D.C. Radford, H. Schnare, P. Vaska, D. Ward, J.N. Wilson, and I. Ragnarsson, *Phys. Rev. C* **53**, 2763 (1996).
- [11] R. Wadsworth, H.R. Andrews, C.W. Beausang, R.M. Clark, J. DeGraaf, D.B. Fossan, A. Galindo-Uribarri, I.M. Hibbert, K. Hauschild, J.R. Hughes, V.P. Janzen, D.R. LaFosse, S.M. Mullins, E.S. Paul, L. Persson, S. Pilotte, D.C. Radford, H. Schnare, P. Vaska, D. Ward, J.N. Wilson, and I. Ragnarsson, *Phys. Rev. C* **50**, 483 (1994).
- [12] D.R. LaFosse, D.B. Fossan, J.R. Hughes, Y. Liang, H. Schnare, P. Vaska, M.P. Waring, J.-y. Zhang, R.M. Clark, R. Wadsworth, S.A. Forbes, E.S. Paul, V.P. Janzen, A. Galindo-Uribarri, D.C. Radford, D. Ward, S.M. Mullins, D. Prévost, and G. Zwartz, *Phys. Rev. C* **50**, 1819 (1994).
- [13] E.S. Paul, C.W. Beausang, S.A. Forbes, S.J. Gale, A.N. James, P.M. Jones, M.J. Joyce, H.R. Andrews, V.P. Janzen, D.C. Radford, D. Ward, R.M. Clark, K. Hauschild, I.M. Hibbert, R. Wadsworth, R.A. Cunningham, J. Simpson, T. Davinson, R.D. Page, P.J. Sellin, P.J. Woods, D.B. Fossan, D.R. LaFosse, H. Schnare, M.P. Waring, A. Gizon, J. Gizon, T.E. Drake, J. DeGraaf, and S. Pilotte, *Phys. Rev. C* **50**, 698 (1994).
- [14] I. Thorslund, D.B. Fossan, D.R. LaFosse, H. Schnare, K. Hauschild, I.M. Hibbert, S.M. Mullins, E.S. Paul, I. Ragnarsson, J.M. Sears, P. Vaska, and R. Wadsworth, *Phys. Rev. C* **52**, R2839 (1995).
- [15] E.S. Paul, C.W. Beausang, S.A. Forbes, S.J. Gale, A.N. James,

- R.M. Clark, K. Hauschild, I.M. Hibbert, R. Wadsworth, R.A. Cunningham, J. Simpson, T. Davinson, R.D. Page, P.J. Sellin, P.J. Woods, D.B. Fossan, D.R. LaFosse, H. Schnare, M.P. Waring, A. Gizon, and J. Gizon, *Phys. Rev. C* **48**, R490 (1993).
- [16] M.P. Waring, E.S. Paul, C.W. Beausang, R.M. Clark, R.A. Cunningham, T. Davinson, S.A. Forbes, D.B. Fossan, S.J. Gale, A. Gizon, J. Gizon, K. Hauschild, I.M. Hibbert, A.N. James, P.M. Jones, M.J. Joyce, D.R. LaFosse, R.D. Page, I. Ragnarsson, H. Schnare, P.J. Sellin, J. Simpson, P. Vaska, R. Wadsworth, and P.J. Woods, *Phys. Rev. C* **51**, 2427 (1995).
- [17] E.S. Paul, H.R. Andrews, V.P. Janzen, D.C. Radford, D. Ward, T.E. Drake, J. DeGraaf, S. Pilotte, and I. Ragnarsson, *Phys. Rev. C* **50**, 741 (1994).
- [18] E.S. Paul, D.B. Fossan, K. Hauschild, I.M. Hibbert, H. Schnare, J.M. Sears, I. Thorslund, R. Wadsworth, A.N. Wilson, and J.N. Wilson, *Phys. Rev. C* **51**, R2857 (1995).
- [19] P.J. Nolan, F.A. Beck, and D.B. Fossan, *Annu. Rev. Nucl. Part. Sci.* **45**, 561 (1994).
- [20] D.C. Radford, *Nucl. Instrum. Methods A* **361**, 297 (1995).
- [21] D.B. Fossan, in *Proceedings of the Workshop on Gammasphere Physics*, Lawrence Berkeley National Laboratory, (World Scientific, Singapore, in press).
- [22] T. Ishii, A. Makishima, M. Shibata, and M. Ishii, *Phys. Rev. C* **49**, 2982 (1994).
- [23] T. Bengtsson and I. Ragnarsson, *Nucl. Phys.* **A436**, 14 (1985).
- [24] S. Frauendorf, *Nucl. Phys.* **A557**, 259c (1993); S. Frauendorf, in *Proceedings of the Workshop on Gammasphere Physics*, Lawrence Berkeley National Laboratory, 1995 (World Scientific, Singapore, in press).
- [25] M. Ionescu-Bujor, A. Iordachescu, G. Pascovici, and C. Stansion, *Nucl. Phys.* **A466**, 317 (1987).